TI Designs

High Efficiency, Versatile Bidirectional Power Converter for Energy Storage and DC Home Solutions

TI Designs

The TIDA-00476 TI Design consists of a single DC-DC power stage, which can work as a synchronous buck converter or a synchronous boost converter enabling bidirectional power flow between a DC power source and energy storage system. Operating in synchronous buck mode, the system works as an MPPT-controlled DC-DC converter, which can charge a battery from a solar panel or DC source. The same power stage can also be operated as a synchronous boost to drive a DC load with configurable constant current and constant voltage (CC-CV) limits from an energy storage system, such as a lead acid battery. The power stage is digitally controlled by a TI MSP430™ microcontroller, which implements the closed loop for controlling the power stage with the required algorithms for MPPT, battery charge profiling, and DC-DC power conversion for a load.

Design Resources

TIDA-00476	Tool Folder Containing Design Files
CSD88539ND	Product Folder
MSP430F5132	Product Folder
LM5109A	Product Folder
UCC28880	Product Folder
OPA170	Product Folder
TLV704	Product Folder

TI E2E™ Community

ASK Our E2E Experts

Design Features

- Single Bidirectional Power Stage Functions as Both Synchronous Buck Battery Charger and Synchronous Boost CC-CV Converter
- High Efficiency of 95% as Charger to Store Energy and 90% as CC-CV Driver to Power Loads
- Perturb and Observe (P&O) Based MPPT Tracking Algorithm
- Robust Power Stage With Built-in Protection for Overcurrent, Overvoltage, and Reverse Polarity Connection
- Fully Tested and Validated as an MPPT-Based Lead Acid Battery Charger and CC-CV Driver With LED and MPPT-Based Loads
- Easy-to-Use PCB Form Factor of 85 x 50 mm
- Provides Ready Platform for Single-Stage Bidirectional Power Conversion Requirements of Energy Storage, DC Home, and Low Power UPS Systems

Featured Applications

- MPPT Solar Battery Charger
- Standalone Solar Street Lights
- DC-UPS Systems
- E-Bikes
- DC Home Applications

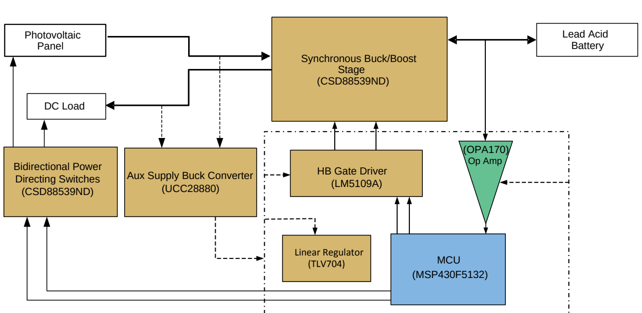

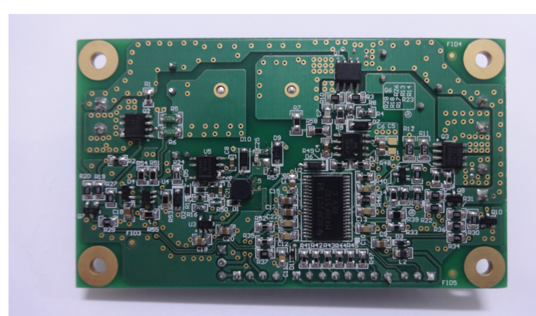

1 Key System Specifications

Table 1. System Specifications

PARAMETERS	SPECIFICATIONS
Panel voltage range	14 V to 44 V
Battery voltage range	12- to 24-V lead acid battery
Battery charging current max	5 A
Load voltage range	45 V
Max load current	700 mA (extendable up to 1.2 A on the same board)
Protection as charger	Battery overcurrent, battery overvoltage, battery reverse polarity, and panel overvoltage
Protection as CC-CV DC-DC converter	Battery deep discharge, load overcurrent, and load overvoltage
Standby power	50 mW
Electrical efficiency	Approximately 95% as battery charger and approximately 90% as CC-CV DC-DC converter
Operating ambient temperature	Up to 55°C
Board form factor	PCB type: FR4, two-layer

2 System Description

Solar powered applications such as standalone solar streetlights require the following system capabilities: a system to charge a lead acid battery from the solar panel and a system to drive the streetlight from the battery. In conventional solutions, establishing these capabilities requires the use of two power stages: one power stage for charging the battery and another for operating as a CC-CV driver. The two power stages can be independently controlled through separate discrete circuits or by using a single digital controller.

By combining the two power stages into a single bidirectional power stage, this TIDA-00476 reference design proposes an optimized solution in terms of performance, cost, and size. The design utilizes a MSP430F5132 microcontroller (MCU) to control the system. This MCU enables the system to implement a maximum power point tracker (MPPT) and a four-stage battery-charging algorithm, which is easy to customize according to the end systems requirements.

3 Block Diagram

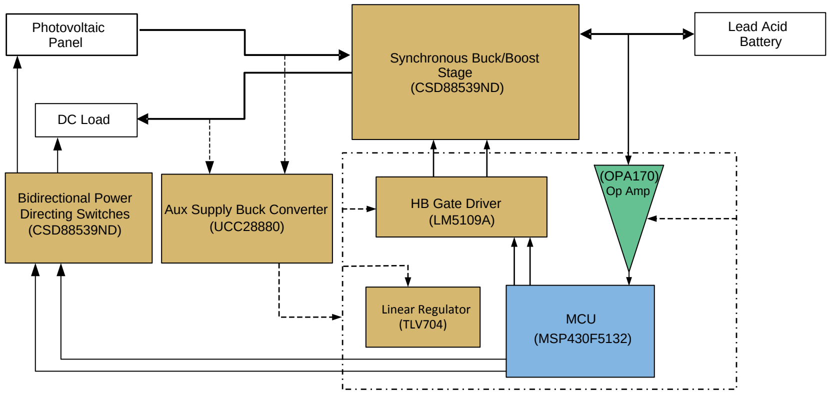

Figure 1. TIDA-00476 Block Diagram

3.1 Highlighted Products

The following are the highlighted products used in this reference design. This section lists the key features for selecting these products. Refer to the respective product datasheets for more device details.

For more information on each of these devices, see the respective product folders at www.ti.com.

3.1.1 MSP430F5132

The Texas Instruments (TI) MSP430™ family of ultralow-power MCUs consists of several devices featuring different sets of peripherals targeted for various applications. The architecture, combined with five low-power modes, is optimized to achieve extended battery life in portable measurement applications. The device features a powerful 16-bit reduced instruction set computing (RISC) processor.

The MSP430F51x2 series of MCUs feature configurations with two 16-bit high-resolution timers, two USCIs (USCI_A0 and USCI_B0), a 32-bit hardware multiplier, a high-performance 10-bit ADC, an on-chip comparator, a three-channel direct memory access (DMA), 5-V tolerant input/outputs (I/O)s, and up to 29 I/O pins. In the TIDA-00476 reference design, the switching frequency of the power stage is set to 100 kHz when operating as a synchronous buck and 350 kHz when operating as a synchronous boost. The high resolution timer, which can run at internally generated clock speeds up to 256 MHz, is very useful for these high PWM frequency applications because the timer is able to run with sufficient duty cycle resolutions, even at 350 kHz.

Apart from the high-resolution Timer_D, the built-in 10-channel analog-to-digital converter (ADC) and DMA meet the requirement of this application.

3.1.2 LM5109A

The losses across a switching MOSFET can be considered as a summation of the conduction losses and the switching losses. While the conduction losses depend greatly on the chosen RDSon of the MOSFET, the switching loss depends on the input capacitance and the gate drive circuit of the MOSFET. The gate drive circuit controls the turnon and turnoff time of the MOSFET.

To reduce the switching losses, the turnoff and turnoff time of the MOSFETs must be minimized. Minimizing this time requires a high-current gate driver.

The LM5109A is a high voltage, half-bridge gate driver with a 1-A peak gate current. The device is capable of operating with rail voltages up to 90 V and is well suited for half bridge and synchronous buck applications. The high gate-drive current reduces the MOSFET switching time, which effectively reduces the losses in the MOSFET and improves the efficiency of the system. The LM5109A device provides two transistor-transistor logic (TTL) compatible input pins, which are connected to the complementary PWM outputs generated from the MSP430 Timer_D. The input at these two pins independently controls the outputs of the LM5109A.

3.1.3 OPA170

The OPA170 is a low-noise precision amplifier with a wide operating voltage range, high bandwidth, and excellent common-mode rejection ratio (CMRR). The OPA170 device can operate on a single supply from 2.7 V to 36 V. This operational amplifier (op amp) has been chosen for its very high CMRR (> 120 dB) and excellent offset, drift properties. The OPA170 is a single op amp, which is available in a micro-package SOT553.

The OPA170 op amp is used in the TIDA-00476 reference design to measure the battery charging current in a differential amplifier configuration where the common-mode input voltage can be very high.

This op amp has a high CMRR and is able to operate over a wide operating voltage range, which makes it quite suitable for this application. This op amp is available in a micro package, which also helps maintain the required board space to a minimum.

For more information on the OPA170 op amp, refer to the product datasheet (SBOS557).

3.1.4 CSD88539ND

The CSD88539ND is a dual N-channel, 60-V, NexFET™ power MOSFET from TI, which is available in a single SO-8 package. The CSD88539ND MOSFET has an extremely low gate charge of 7.2 nC at 10 V and a RDSon of 23 mΩ. This MOSFET is very suitable for low-voltage half-bridge applications.

The CSD88539ND meets the application requirements specified for the TIDA-00476 design because of its very low gate charge and RDSon, which minimizes the losses in the switching stage.

3.1.5 UCC28880

The UCC2880 is a versatile offline controller with an integrated 700-V MOSFET. The device can be used to build AC-DC or DC-DC converters based on most of the common topologies such as buck, buck-boost, flyback, and so forth with a minimal number of external components.

The UCC2880 device has a low quiescent current and enables the designer to achieve good efficiency while building low power AC-DC or DC-DC converters using this IC.

In this application, a buck converter based on the UCC288800 is used to develop the 10-V bias supply.

3.1.6 TLV70433

The TLV704 series of low-dropout (LDO) regulators are ultralow quiescent current devices designed for extremely power-sensitive applications. Quiescent current is virtually constant over the complete load current and ambient temperature range.

The TLV704 operates over a wide operating input voltage of 2.5 V to 24 V. The TLV704 is available in a 3-mm × 3-mm SOT23-5 package, which is ideal for cost-effective board manufacturing.

In the TIDA-00476 board, the TLV074 device is used to supply a regulated 3.3 V to the MSP430F5132 device.

4 System Design Theory

The versatile bidirectional power supply is an integration of two systems: a DC-DC synchronous buck converter for charging a lead acid battery and a DC-DC synchronous boost converter for driving a CC-CV DC load from the lead acid battery.

Control of the system is managed through an onboard MSP430F5132 microcontroller. The firmware running on the MSP430F5132 implements the closed loop for the power stage along with the algorithms required for implementing MPPT control, battery charge profiling, and CC-CV for the CC-CV DC-DC driver.

The key differentiation in this design is the fact that a single power stage functions as both synchronous buck and synchronous boost converters. The firmware running on the MSP430F5132 determines when to operate the power stage as a synchronous buck converter or a synchronous boost converter.

Upon closer examination of the synchronous buck power stage, it is noticeable that by reversing the role of the two MOSFETs the synchronous buck stage can be converted into a synchronous boost stage. This property of the synchronous buck power stage allows the designer to implement the bidirectional power flow controller.

The following Figure 2 and Figure 3 show the power flow when the power stage is working as a synchronous buck and synchronous boost converter.

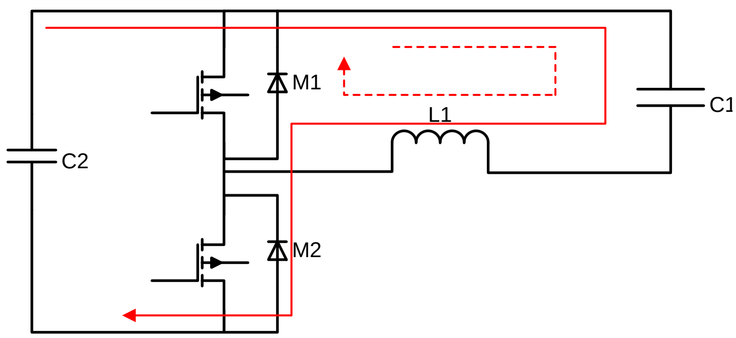

Figure 2. Power Stage When Working as Synchronous Buck Converter

When working as a synchronous buck converter, the Q1A MOSFET functions as the main switching MOSFET. When this MOSFET is on, power flows from the solar panel, through the battery, through the inductor, and then returns to the solar panel. The bold red line without dashes in Figure 2 shows this power flow path. The Q1B MOSFET functions as the synchronous MOSFET. After turning off the Q1A MOSFET, the current that passes through the inductor freewheels through the battery and the body diode of the Q1B MOSFET. After a small dead time the Q1B MOSFET is turned on allowing for the inductor current to flow through the body of Q1B. The dashed red line in Figure 2 shows this power flow path.

When working as a synchronous boost converter, the Q1B MOSFET functions as the main switching MOSFET. When this MOSFET is on, power flows from the battery into the inductor and returns to the battery. The bold red line without dashes in Figure 3 shows this power flow path. The Q1A MOSFET functions as the synchronous MOSFET. On turning off Q1B current through the inductor charges the output capacitors C2 and C3, goes through the battery and the body diode of Q1A. After a small dead time the Q1A is turned on allowing for the inductor current to flow through the body of Q1A. The dashed red line in Figure 3 shows this power flow path.

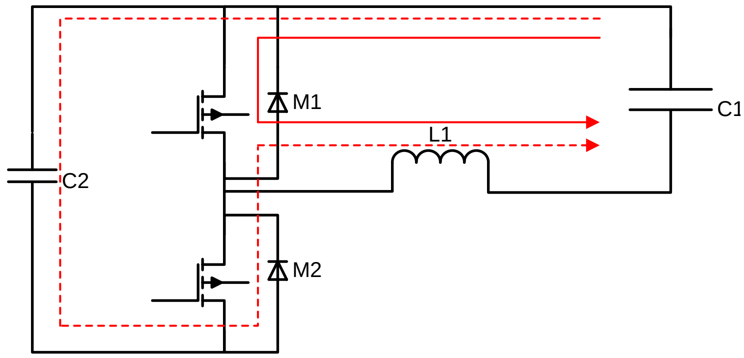

Figure 3. Power Stage When working as a Synchronous Boost Converter

The system has two modes of operation, the battery charging mode and the CC-CV DC-DC converter mode. During the charging mode, the MCU runs the required control loops to operate the power stage as a synchronous buck converter and provides a four-stage charging profile for the battery. In the CC-CV DC-DC driver mode, the MCU runs the control loops to operate the synchronous boost converter to maintain the CC-CV operation.

The system provides protection features such as battery and panel reverse polarity connection prevention, overcurrent, overvoltage, and so forth.

The following subsections provide an overview of the systems working in both battery charging mode and CC-CV driver mode. To include the explanation for the MPPT-related features of the system, the battery charging functionality is explained in the scenario where charging is accomplished with a PV panel and not with a DC source. When the battery is charged from a DC source, all features remain enabled, but the MPPT has no impact.

4.1 System as MPPT Battery Charger

While functioning as a battery charger, the MSP430F5132 device operates the power stage in the synchronous buck configuration. The system is capable of charging a 12-V lead acid battery from a photovoltaic (PV) panel with an open circuit voltage from 15 V to 44 V or a DC source.

The MSP430F5132 device implements the necessary algorithm for extracting maximum power from the photovoltaic panels and charging the lead acid battery using a four-stage charging profile.

The power output from a PV panel depends on a few parameters, such as the irradiation received by the panel voltage, panel temperature, and so forth. The power output also varies continuously throughout the day as the conditions affecting it change.

The following Figure 4 shows the I-V curve and the P-V curve of a solar panel. The I-V curve represents the relationship between the panel output current and its output voltage. As the I-V curve in the figure shows, the panel current is at the maximum when its terminals are shorted and is at its lowest when the terminals are open and unloaded.

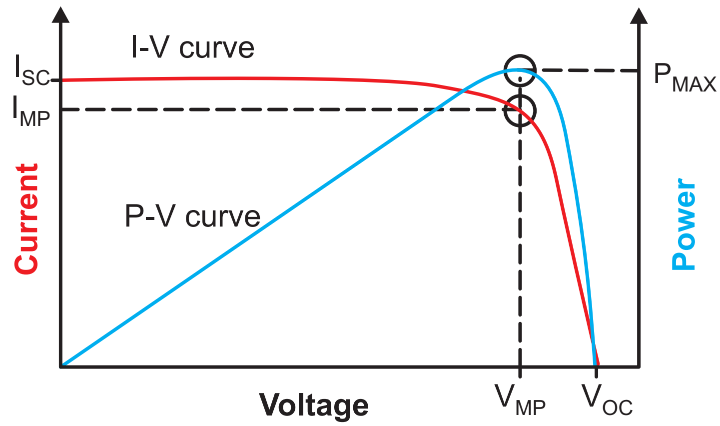

Figure 4. Solar Panel Characteristics I-V and P-V Curves

As the preceding Figure 4 shows, the user can obtain the maximum power output from the panel represented as P_{MAX} at a point when the product of the panel voltage and the panel current is at the maximum. This point is designated as the maximum power point (MPP).

The following graphs in Figure 5 and Figure 6 show examples of how each of the various parameters affect the output power from the solar panel. The graphs also show the variation in the power output of a solar panel as a function of irradiance. Observe in these graphs how the power output from a solar panel increases with the increase in irradiance and decreases with a decrease in irradiance. Also note that the panel voltage at which the MPP occurs also shifts with the change in irradiance.

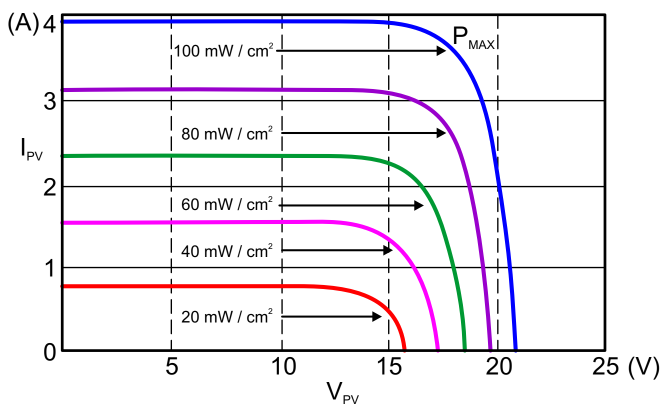

Figure 5. Solar Panel Output Power Variation Under Different Irradiation Conditions—Graph A [2]

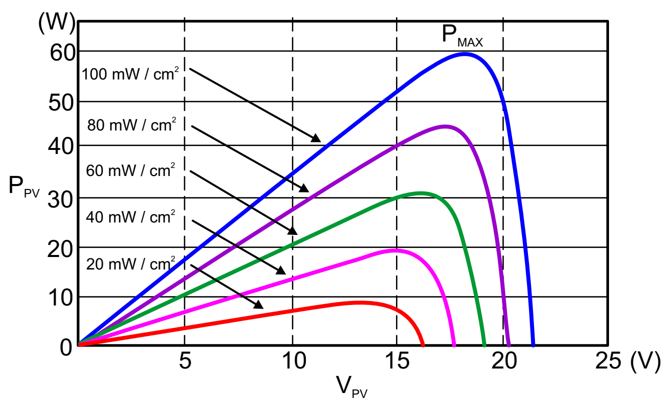

Figure 6. Solar Panel Output Power Variation Under Different Irradiation Conditions—Graph B [2]

Figure 7 shows a typical graph representing the variation in the power output of a photovoltaic panel as a function of its temperature. Observe how the panel current (and thereby the panel power) decreases with an increase in temperature. The MPP voltage continues to shift substantially with the change in temperature.

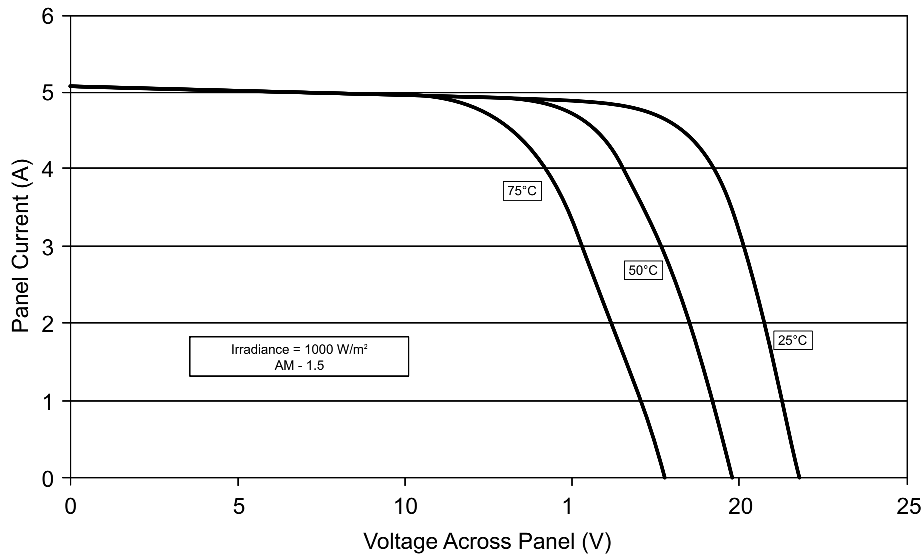

Figure 7. Solar Panel I-V Curve Variation With Temperature Under Constant Irradiation Conditions

The user can draw the maximum power from a solar panel by operating the panel close to the MPP point; however, doing so poses two challenges:

1. Providing a way to connect a battery or load with a different operating voltage in comparison to the MPP of the panel
2. Identifying the MPP automatically, as it varies with the environmental conditions and is not a constant

Directly connecting a solar panel with a V_{MPP} close to 17 V to a 12-V lead acid battery forces the panel to operate at 12 V, which reduces the amount of power that can be drawn from the panel. From this situation, the user can surmise that a DC-DC converter is able to draw more power from the solar panel because this converter forces the solar panel to operate close to the V_{MPP} and transfer the power to a 12-V lead acid battery (impedance matching).

The preceding paragraph explains why the user implements a synchronous buck converter to charge the lead acid battery from the solar panel and address the first challenge.

The second challenge of automatically identifying the MPP of the panel is typically performed by employing MPPT algorithms in the system. The MPPT algorithm tries to operate the photovoltaic panel at the maximum power point and uses a switching power stage to supply the load with the power extracted from the panel.

There are many variations of the MPPT algorithm available. The following list shows four of the most widely used algorithms:

- Perturb and observe
- Incremental conductance
- Fractional open-circuit voltage
- Fractional short-circuit current

The following subsections provide a brief description of each of these algorithms.

4.1.1 Perturb and Observe (P&O)

Perturb and observe is one of the most popular MPPT algorithms used. The fundamental principle behind this algorithm is simple and easy to implement in a microcontroller based system. The process involves slightly increasing or decreasing (perturbing) the operating voltage of a panel. Perturbing the panel voltage is accomplished by changing the duty cycle of the converter. Assuming that the panel voltage has been slightly increased and that this leads to an increase in the panel power, then another perturbation in the same direction is performed. If the increase in the panel voltage decreases the panel power then a perturbation in the negative direction is done to slightly lower the panel voltage.

By performing the perturbations and observing the power output, the system begins to operate close to the MPP of the panel with slight oscillations around the MPP. The size of the perturbations determines how close the system is operating to the MPP. Occasionally this algorithm can become stuck in the local maxima instead of the global maxima, but this problem can be solved with minor tweaks to the algorithm.

The P&O algorithm is easy to implement and effective.

4.1.2 Incremental Conductance

Incremental conductance works by calculating the change induced in the panel current when a small change in the panel voltage is performed. This algorithm depends on the fact that ΔI_{PANEL} / ΔV_{PANEL} has a value of 0 when operating at the MPP. As a result, when at the MPP, this algorithm can work without further oscillations as long as the environmental conditions do not vary.

By measuring the panel current and panel voltage and comparing these measurements with ΔI_{PANEL} / ΔV_{PANEL}, the algorithm can detect whether it is operating at the right or left of the MPP and move in the correct directions.

4.1.3 Fractional Open-Circuit Voltage

Fractional open-circuit voltage operates based on the fact that, for most panels, the voltage at the MPP (V_{MP}) is between 0.7 to 0.8 times the open-circuit voltage (V_{OC}). By periodically measuring the open-circuit voltage , the algorithm can adjust the operating point to force the panel to operate between 0.7 to 0.8 times the V_{OC}.

This method is very simple to implement but the drawback is that the power stage must be periodically disconnected to measure the panel V_{OC}. Another issue with this algorithm is the minor panel-to-panel variation in the relationship between V_{MP} and V_{OC}

4.1.4 Fractional Short Circuit Current

The fractional short circuit current algorithm operates in a similar way to the fractional open-circuit voltage algorithm. Fractional short circuit current is different in that it uses the short circuit current I_{SC} as an estimate for the I_{MPP}. The fractional short circuit current adjusts the operating point until the current from the panel is close to the I_{MPP}.

Fractional short circuit current suffers from the same drawback as the fractional open circuit voltage-based system, which is that the panel must be disconnected periodically. Additionally, the fractional short circuit current system requires a provision for shorting it and measuring the current.

The P&O MPPT algorithm has been used in this system, as it is relatively easier to implement and very effective in tracking the maximum power point accurately. For these reasons, it is one of the most popular MPPT algorithms used.

Lead acid batteries require a three-stage charging process with an optional fourth stage. The three major stages involved in charging a lead acid battery are known as the bulk stage, absorption stage, and float stage. The optional fourth stage is only required when charging a deep-discharge lead acid battery.

The following Figure 8 shows the various stages involved in charging a lead acid battery including the battery voltage and charging current in each stage.

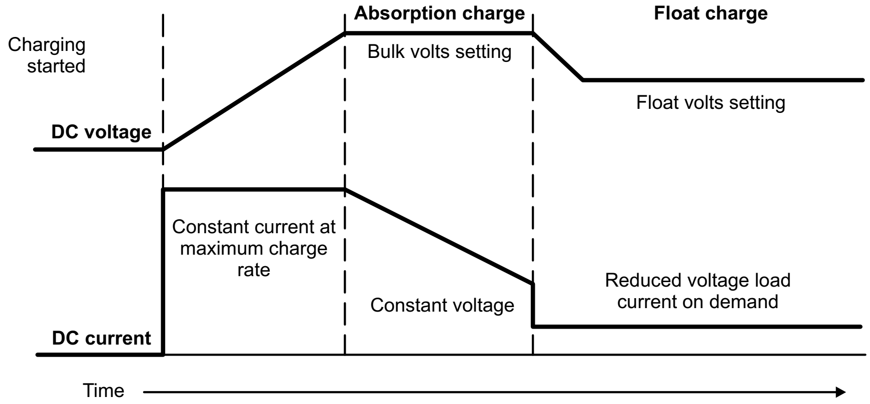

Figure 8. Lead Acid Battery Charging Stages

In the bulk charging stage, the battery is charged with a constant current of C/10 to C/5 until the battery reaches a predetermined maximum charging voltage. The value of the maximum charging voltage is specific to the type of lead acid battery. For example, for a 12-V battery, this maximum charging voltage can range between 14.2 V to 14.8 V. During the bulk charging stage, the battery is charged up to 80% of its full capacity.

In the absorption stage, the battery is maintained at a constant voltage equal to the maximum charging voltage specified for the battery. The charging current required to maintain the battery at this maximum charging voltage tapers down slowly until it reaches a minimum value. At this point, the battery is assumed to be charged to its full capacity.

When the battery is fully charged, it remains charged by float charging. Float charging is necessary to compensate for the self-discharge of the lead acid battery. Float charging is performed by keeping the battery at a constant voltage, which is lower than the maximum charging voltage of the battery. Float charging keeps the battery at the full charge and avoids damage to the battery, which can result from maintaining the battery at the maximum charging voltage. This measure increases the life of the battery while maintaining the battery charge at the maximum capacity.

The implementation of the synchronous buck converter in the TIDA-00476 design is slightly different from that of a traditional implementation. In this system, the power stage has two additional modes of operation when configured as a synchronous buck stage. The power stage can either operate in synchronous buck mode or in diode emulation mode.

Diode emulation is the process by which the internal body diode of a MOSFET is used in the place of an external Schottky diode in a buck converter. The following Figure 9 shows the flow of current in both modes. The solid line represents the power flow in the synchronous buck mode and the dashed line represents the power flow in diode emulation mode.

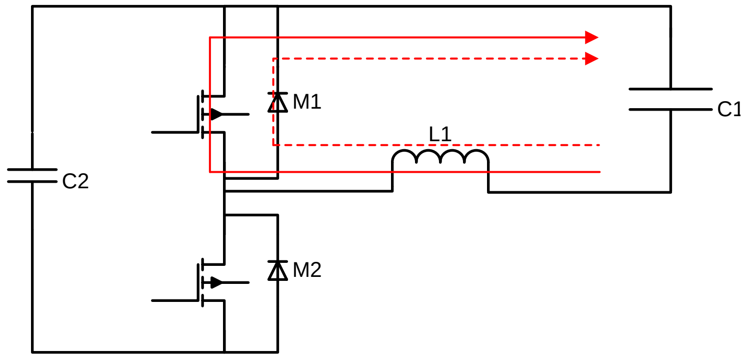

Figure 9. Synchronous Buck Power Stage in Synchronous Buck and Diode Emulation Modes

The efficiency of the system can be improved by operating the synchronous buck stage in diode emulation mode under low-load conditions. Under low-load conditions, the average inductor current is typically low. As a result of this low average current, the instantaneous inductor current can go negative there by increasing the RMS current and reducing the converter efficiency (if operated in synchronous buck mode). In diode emulation, the system enters discontinuous conduction mode DCM and the root mean square (RMS) current can be lowered here by giving better efficiency. Another advantage of operating in diode emulation mode with low loads is that the user can stop the battery from accidentally dumping the power into the panel.

In the current system, when the battery current decreases to less than 1 A, the synchronous buck power stage begins operating in diode emulation mode. When the current increases above 1.2 A, the system switches back to working in the synchronous buck mode.

4.2 System as Boost Converter for DC-DC Loads

When there is no power transfer from the solar panel, the power stage is configured by the MSP430 device to work as a synchronous boost converter.

As a synchronous boost converter, the system can drive a DC load up to 45 V and 1-A current with close to a 92% efficiency level. This system works as a CC-CV limited power supply with configurable CC and CV limits. The system is especially suitable for DC loads that must be driven in CC mode, such as LED string and so forth.

The control components of the synchronous boost converter are implemented using the MSP430 device. The MSP430 device generates the required pulse width modulation (PWM) using the internal timer and takes the load voltage and load current as feedback through the ADC. The load voltage and load current information obtained are then used to control the PWM duty cycle to implement CC-CV control of the converter.

4.3 Power Stage Component Selection

The MSP430 device controls the operation of the power stage. The switching frequency of the power stage when operating as a synchronous buck converter is 100 kHz. When operating as a synchronous boost converter, the switching frequency is 350 kHz. The difference in the switching frequency is because of the fact that the power stage components must remain the same while working as a synchronous buck or boost converter.

The following subsections detail the design goal parameters. These parameters are used to explain the selection of various important components.

4.3.1 Inductor L1

Selection of the inductor L1 is primarily determined by the allowable ripple current. In this system, the buck converter specifications are used to derive the inductor ripple current requirements. The following calculation in Equation 2 assumes a maximum panel voltage of 44 V:

$$I_{RIPPLE\_BUCK} = 0.4 \times I_{CHARGER\_MAX} = 2\ A$$

$$D_{MIN\_BUCK} = \frac{V_{BAT\_MIN}}{V_{PANEL\_MAX}} = \frac{10}{44} = 0.227 \tag{1}$$

$$I_{RIPPLE\_BUCK} = \frac{\left(V_{PANEL\_MPP} - V_{BAT\_MIN}\right)}{F_{SW\_BUCK} \times L1} \tag{2}$$

Rearranging and solving for the inductor value results in Equation 3:

$$L1 = 38.6\ \mu H \tag{3}$$

An Inductor value of 47 uH has been chosen for use as L1.

By substituting the value of L1 in the preceding Equation 2, the actual value of the I_{RIPPLE_BUCK} can be computed in Equation 4:

$$I_{RIPPLE\_BUCK} = 1.64\ A \tag{4}$$

By using the value of inductor in Equation 4 to estimate the ripple current through it when the system is operating as a boost converter results in Equation 5:

$$I_{RIPPLE\_BOOST} = V_{BAT\_MIN} \times \frac{D_{MAX\_BOOST}}{L1 \times F_{SW\_BOOST}} \tag{5}$$

To calculate the value for D_{MAX_BOOST}, use the following Equation 6:

$$D_{MAX\_BOOST} = 1 - \frac{V_{BAT\_MIN}}{V_{LOAD}} = 0.77 \tag{6}$$

Substitute the D_{MAX_BOOST} value from Equation 6 into Equation 5 to obtain an I_{RIPPLE_BOOST} = 0.47 A.

From the ripple current calculations, the user can estimate the minimum current rating of the MOSFET that must be used in the power stage.

4.3.2 Capacitor C2 and C3

When operating as a battery charger, capacitors C2 and C3 are the input capacitors for the system.

The selection of the input capacitors depends on the voltage ripple that can be allowed on the input. Because the system is working as a buck converter, the input voltage ripple tends to be a bit higher. Generally this higher ripple is allowed to be up to 5-10% of the input voltage.

When the system is working as a synchronous boost converter, capacitors C2 and C3 become the output capacitors of the system. The requirements for capacitors C2 and C3 are derived based on this mode.

The primary contributor to the output voltage ripple is the equivalent series resistance (ESR) of the capacitors in parallel and the ripple current through it. In this design, two 390-µF capacitors are placed in parallel with a combined ESR of 75 mΩ.

Equation 7 calculates the output ripple:

$$V_{OUT\_RIPPLE} = ESR \times \left(\frac{I_{OUT\_MAX}}{1 - D_{MAX\_BOOST}} + \frac{I_{RIPPLE\_BOOST}}{2} \right) + I_{OUT\_MAX} \times \left(\frac{D_{MAX\_BOOST}}{F_{SW\_BOOST} \times (C2 + C3)} \right) \tag{7}$$

Substituting the values of capacitance and the corresponding ESR in the preceding Equation 7 along with the values for duty cycle and current results in a V_{OUT_RIPPLE} = 250 mV, which is a value within the acceptable limits.

4.3.3 Capacitor C1

Capacitor C1 is the output capacitor of the system when the system is working as a battery charger. C1 along with L1 form the output filter and its value is crucial in determining the output voltage ripple experienced by the battery.

Selecting a capacitor with a sufficient ripple current rating and low ESR is important to obtain an adequate performance.

The expression for the output voltage ripple in a buck converter as a function of the capacitance of the capacitor and ESR is expressed in the following Equation 8:

$$V_{BAT\_RIPPLE} = \frac{I_{RIPPLE\_BUCK}}{8 \times F_{SW\_BUCK} \times C1} + ESR \times I_{RIPPLE\_BUCK} \tag{8}$$

This design implements a 390-µF capacitor with a 150-mΩ ESR, which leads to a ripple voltage at capacitor C1 equal to 250 mV. At the highest input voltage, when I_{RIPPLE_BUCK} is at its highest, a ripple voltage of 250 mV at the output is within acceptable limits.

4.4 Battery Current Sense

A closer look at the power stage that Figure 10 shows reveals that this system uses a slightly modified version of the synchronous buck power stage. The system ground is connected to the low-side MOSFET source pin, but the battery terminals are not referenced to the system ground. The battery terminals are actually floating with respect to the system ground.

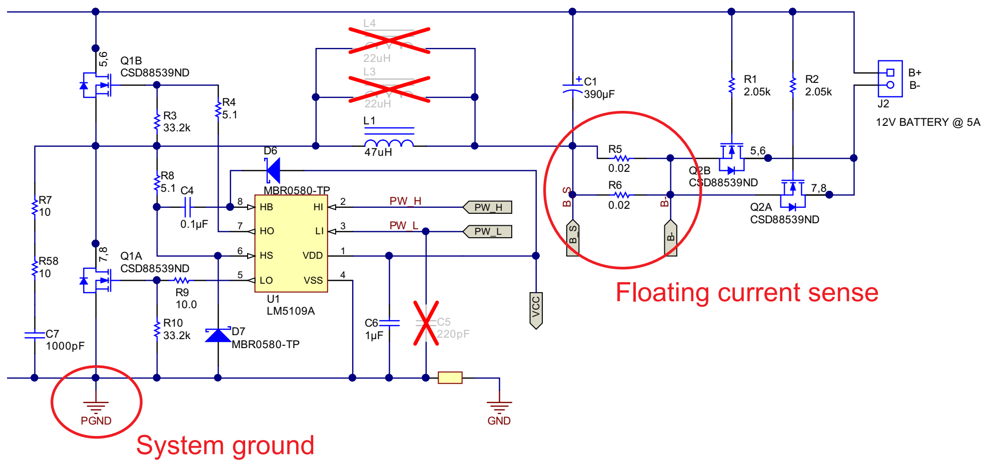

Figure 10. Floating Inputs for Battery Current Sensing

To sense the charging current through the battery, an op amp with a high CMRR is required to reject the high common-mode voltage that can appear across the op amp input terminals. The OPA170A op amp is used in the differential amplifier configuration to perform the current sensing.

The differential voltage generated across the op amp input terminals is proportional to the parallel combination of the current sense resistors (R5 and R6).

4.5 Panel and Battery Voltage Measurement

As earlier sections have explained, the battery connector is floating with respect to the system ground. The battery voltage cannot be directly measured through the MSP430F5132 ADC because it is floating voltage. To measure the battery voltage, a PNP transistor-based circuit is used to convert the battery voltage into an equivalent current flowing through resistor R29. The potential difference across R29 that this current leads to is used to indirectly measure the battery voltage (see Figure 11).

When considering the panel voltage, the panel can either be connected to the system ground or floating depending on the condition of the bidirectional flow control switches. To be able to measure the panel voltage in both conditions, a similar circuit to what was used to measure the battery voltage is used.

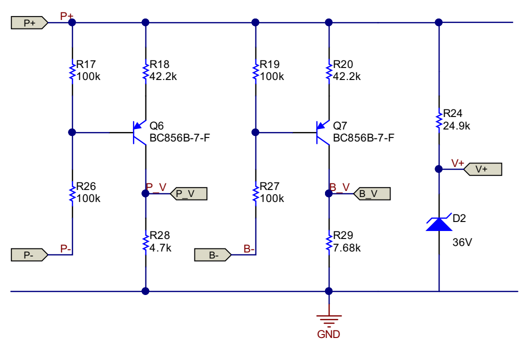

Figure 11. Battery and Panel Voltage Measurement Circuit

4.6 Bias Power Supply

A UCC28880-based buck converter is used as the bias power supply to generate the 10-V supply in this system (see Figure 12). The 10 V generated is used to power the LM5109A gate driver and also to derive the 3.3 V required to power the MSP430F5132.

The bias power supply must generate the 10-V supply from a wide input voltage range of 10.5 V to 55 V. With an integrated, high-voltage MOSFET, the UCC28880 provides a cost effective and efficient option for use in this application.

The UCC28880 is used in a high-side floating buck configuration. Because the internal high-voltage current source for supplying the IC only turns on the IC when the input voltage crosses 30 V, the IC is directly powered from the input voltage at start-up and then the power required to run this IC is drawn directly from the output.

The maximum duty cycle of the UCC28880 is limited to 55%. The value of the inductor and output capacitor have been selected to always run the bias power supply in DCM so as to accommodate such a wide variation in the input voltage and still maintain output voltage regulation.

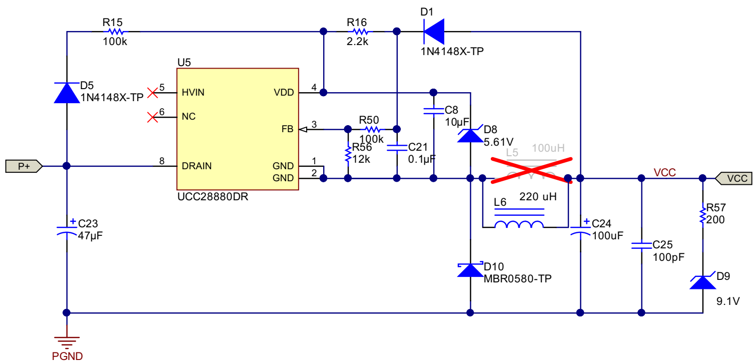

Figure 12. UC28880-Based Auxiliary Supply

4.7 Bidirectional Power Directing Switches

As discussed in previous sections, the direction of power flow in this system is towards the battery when the system is configured as a synchronous buck. The power flow then reverses when the system is configured as a synchronous boost.

When the power flow direction is reversed (that is, the power flow stems from the battery), the user must prevent the system from dumping the power into the panel. To prevent this occurrence, use two MOSFETs as switches to direct the power flow.

The following Figure 13 shows a snapshot of the relevant section in the schematic.

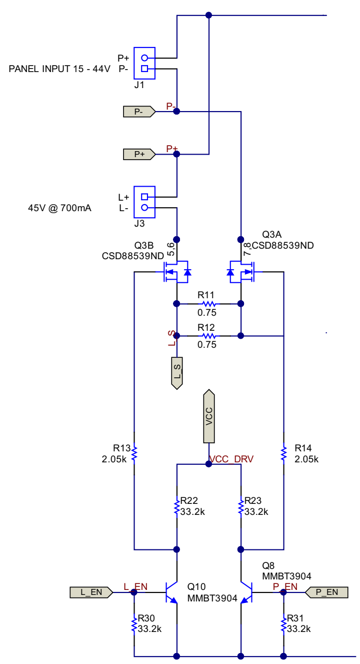

Figure 13. Bidirectional Power Directing Switches

The purpose of the two switches is to channel the flow of power from the panel or to the load depending on the state of the system.

When the system is in the battery charging state, MOSFET Q3A is turned on and MOSFET Q3B is turned off. Power flow occurs from the panel to the battery. As the user can observe, if Q3A is turned off, the power flow is not able to travel in the reverse direction (that is, from the battery to the panel), because the internal diode of the MOSFET blocks the flow.

When the system is in the CC-CV driver state, MOSFET Q3B is turned on and Q3A is turned off. Now the power flows from the battery to load.

The MOSFET switches Q3A and Q3B are controlled through the MSP430 device. Depending on the panel voltage conditions and battery voltage conditions (sensed through the ADC), the MSP430 controls the state of the switches Q3A and Q3B to enable either battery charging or the CC-CV driver.

4.8 Reverse Polarity Protection

The system implements battery reverse polarity protection. This feature protects the system from failure when the battery is accidently connected in reverse at the battery terminal. Figure 14 shows the section of the schematic responsible for implementing this feature. As the schematic shows, the body diodes of MOSFETs Q2A and Q2B automatically become reverse biased if the battery is accidentally connected in reverse priority. This protective measure isolates the battery from the rest of the system.

If the battery is connected with the correct polarity, MOSFETs Q2A and Q2B are turned on by the pullup provided to their gates through resistors R1 and R2, which effectively connects the battery to the rest of the system.

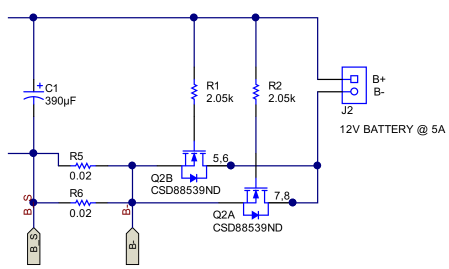

Figure 14. Battery Reverse Polarity Protection

4.9 Firmware

As highlighted in the previous sections, the control loops for the power stage and associated algorithms are implemented using the MSP430F5132.

The MSP430F5132 device measures various parameters on the board through the ADC and then generates the required PWM to control the power stage operation.

The following Figure 15 shows the interaction of the MSP430F5132 with the entire system.

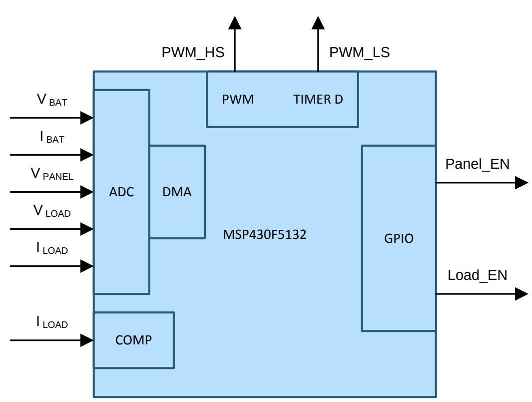

Figure 15. Block Diagram Showing MSP430 Interaction With System

The internal ADC of the MSP430F5132 device is configured to sample five analog signals, specifically the battery voltage, battery current, panel voltage, load voltage, and load current. The internal ADC is used to efficiently sample these analog signals. The use of this internal DMA permits the controller to perform other operations while the ADC is sampling these signal and storing the results in the controller memory.

The bidirectional power stage operates at a 100-kHz switching frequency when working as a synchronous buck and operates at a 350-kHz switching frequency when working as a synchronous boost. The power stage also requires two complementary PWM outputs with sufficient dead time in between them to properly work.

To generate the high-frequency PWM with sufficient resolution, the Timer_D is used in high-resolution mode. Timer_D is internally operated at 200 MHz, which generates the PWM at the frequency this design requires with excellent resolution. To generate a complementary signal with a configurable dead time in between, two instances of Timer_D (TD0 and TD2) are synchronized in master-slave configuration.

Two GPIOs are used to control the bidirectional power-directing switches. Depending on the state of these switches, either the panel or the DC load connect to the system.

Figure 16 shows the overall state diagram, which shows the various states in the firmware and their transitions. The major states in the state machine are:

- Battery charging
- CC-CV driver
- Standby

Apart from these states, a few low-power states (LPM3 and LPM4) exist that the MCU enters into to conserve the standby power of the system. An intermediate state called the load transition state is used to move from the CC-CV driver state to the battery charging state and vice versa. This intermediate state assists in putting the system in a safe mode of operation during transitions.

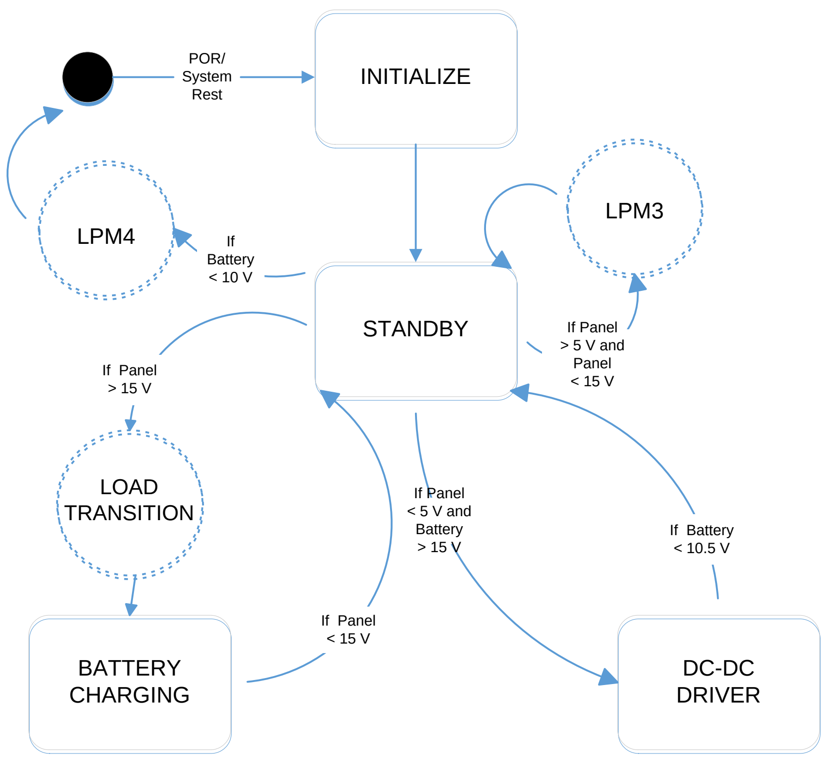

Figure 16. Firmware State Machine

The state machine executes as a part of the main loop of the program. Under normal operating conditions the state machine is executed once every 10.4 ms. When in low-power mode LPM3, the main loop is executed once every two seconds to reduce power consumption.

While operating in the battery charging state, the system charges the lead acid battery. In this state, the system executes a set of functions that regulate the battery voltage and current to follow the required battery profile. Functions for implementing the P&O MPPT are also invoked inside this state.

Figure 17 shows a flowchart of the firmware executing the flow inside this battery charging state. The major functions invoked in this state are:

- GlobalSearch()
- MPPT()
- HoldCC()
- HoldCV()
- UpdateDutyBuck()

The GlobalSearch() function is invoked during the start-up of this state to initially obtain a good estimate of the maximum power point (MPP) of the solar panel. The MPPT() function is invoked periodically. This function implements the P&O MPPT algorithm and keeps the system operating close to the MPP of the panel.

If the available panel power is more than what is required to charge the battery, it is not preferable to operate the panel at the MPP. In this condition, either the HoldCC() or HoldCV() is invoked depending upon the state of the battery. These functions implement the closed loop for keeping the battery charging current and voltage at the preset point. If under any condition the panel power drops below the required power to charge the battery, the MPPT() function is invoked to shift the system operating point close to the MPP of the panel.

The UpdateDutyBuck() function updates the duty cycle of the synchronous buck power stage. This function determines whether to operate the power stage in synchronous buck or diode emulation mode. This determination is made based on the battery charging current. If the current is greater than 1 A, the power stage operates in synchronous buck mode; if the current is less than 1 A, the power stage is operated in diode emulation mode. This setting has been implemented to improve the efficiency when the battery current is low.

There are other system related functions that are invoked in this state. Refer to the *main.c* file in the firmware folder for more details.

Figure 17 shows the flow chart for the battery charging state.

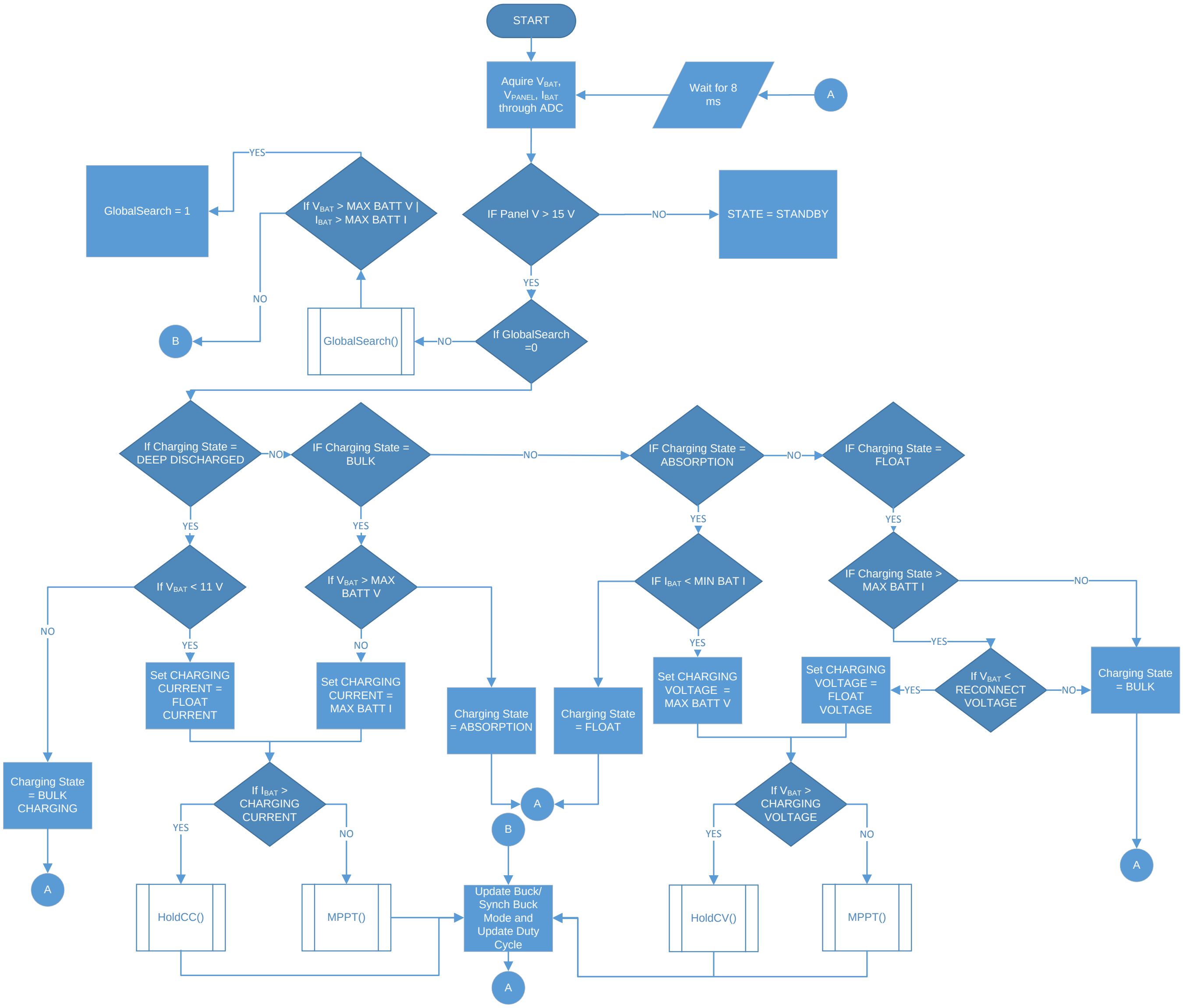

Figure 17. Flow Chart for Battery Charging State

While operating in the CC-CV driver state, the system drives a load from the lead acid battery. In this state the MSP430F5132 device executes a set of functions for regulating the load voltage and current.

Figure 18 shows a flowchart of the firmware executing the flow inside this state. The major functions invoked in this state are:

- LoadRegulateCC()
- LoadRegulateCV()
- LoadManagement()
- UpdateDutyBoost()

The LoadRegulateCC() function is called to regulate the load current to work at the set CC limit. In situations where the load voltage increases beyond the set CV limit, the system begins to regulate the load voltage to work at the CV limit. This regulation is done by invoking the LoadRegulateCV() function. Now when the load current increases to reach the CC limit, the system goes back to the CC-limited operation. The UpdateDutyBoost() function updates the duty cycle of the power stage.

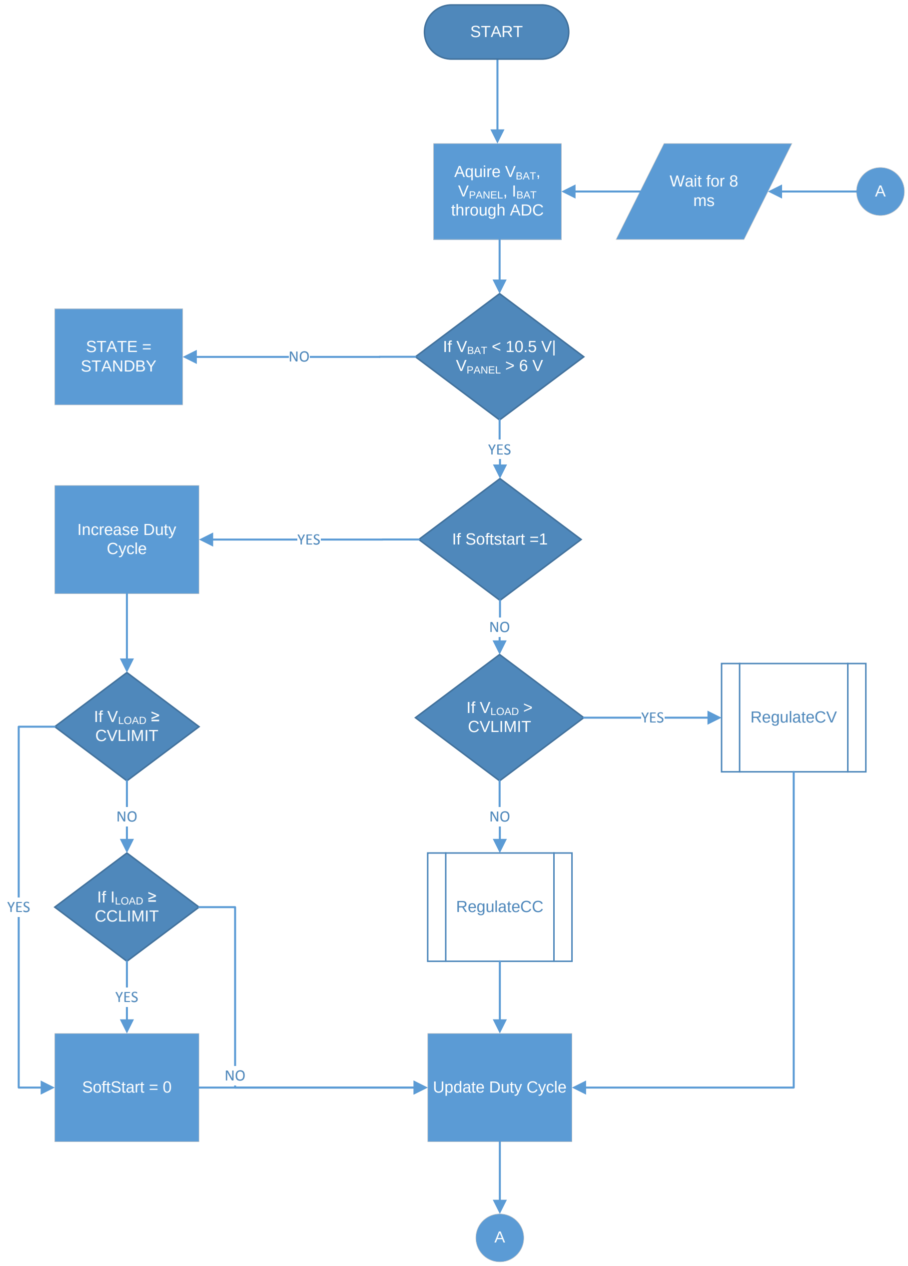

Figure 18. Flow Chart for CC-CV Driver State

The five analog signals battery current (I_{BAT}), battery voltage (V_{BAT}), panel voltage (V_{PANEL}), load voltage (V_{LOAD}), and load current (I_{LOAD}) are acquired through the in-built 10-channel ADC of the MSP430F5132 device. To acquire these signals periodically, the watchdog timer (WDT) is configured to generate an interrupt once every 1.3 ms.

The interrupt routine of the WDT triggers the ADC to start sampling and converting the five ADC signals and stores the data in the controller memory through the DMA controller. When all five signals are converted and stored in the memory, the DMA issues an interrupt to the processor and the command execution shifts to the DMA interrupt routine.

When the system is working in the battery charging state or the CC-CV driving State, the DMA interrupt occurs once every 1.3 ms. The DMA interrupt controls the execution frequency of the main loop. On every eighth DMA interrupt, a 10-ms flag is set in the interrupt routing. This flag controls the execution of the main loop.

If the system is in the standby state, then the watchdog interrupt is configured to occur once every 256 ms, which lowers the frequency of execution of the main loop to once every two seconds.

The following Figure 19 shows the sequence of steps that are executed in the DMA interrupt routine.

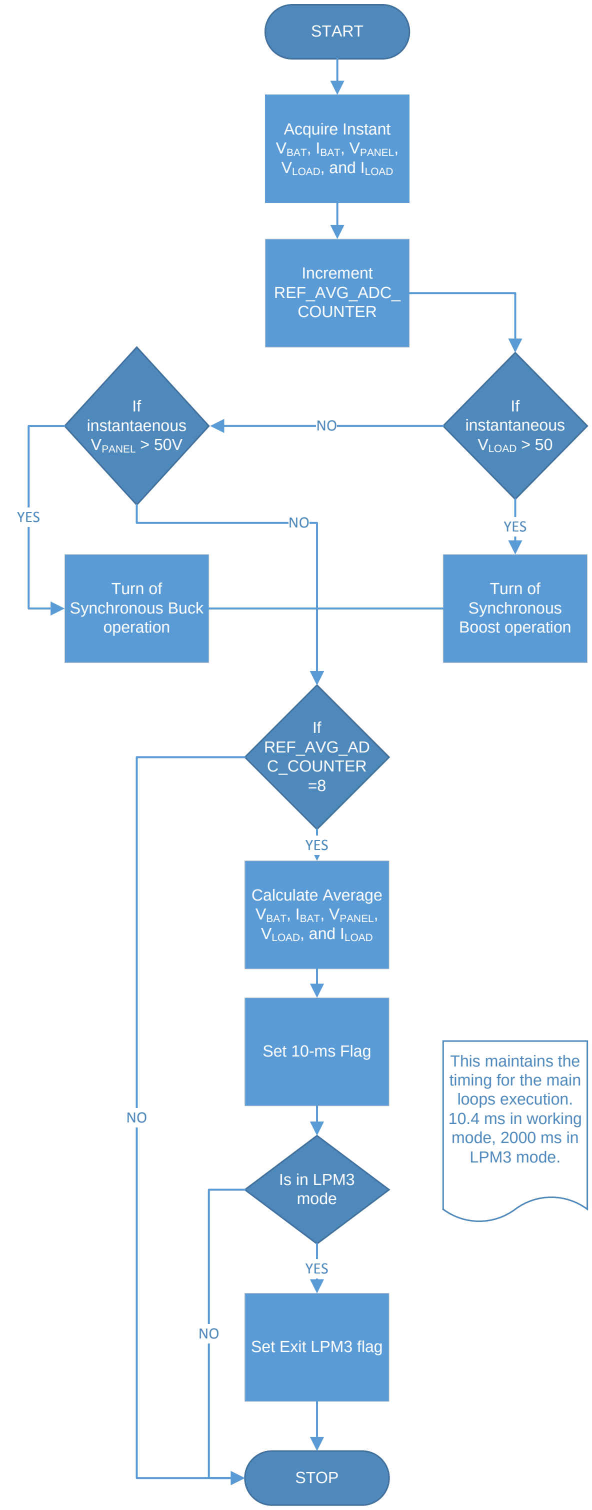

Figure 19. Flow Chart of the DMA Interrupt Service Routine

5 Getting Started Hardware

5.1 Test Conditions

To test the TIDA-00476 board, a DC power supply (acting as a solar panel), 12-V lead acid battery, and electronic load or resistive/LED load is required. The DC power supply must be capable of supplying up to 44 V and 5 A.

5.2 Required Equipment

- DC source
- Lead acid battery
- Digital oscilloscope
- Multimeters
- Electronic load, resistive load, or light-emitting diode (LED) load

5.3 Procedure

1. Connect the panel terminal of the board to the DC source, making sure to maintain the correct polarity.
2. Connect the battery terminal of the board through an ON/OFF switch to maintain the correct polarity.
3. Connect the electronic, resistive, or LED load to the load terminals. In the case of an electronic or resistive load, be sure to maintain the correct polarity.
4. Keeping the DC power supply OFF, turn on the battery switch.
5. The TIDA-00476 board then acts as a CC-CV driver and supplies the load.
6. Observe the startup and continuous waveforms.
7. Turn on the DC supply with a set voltage greater than 15 V and with the CC limit set to almost 1 A.
8. The board then ceases to work as a CC-CV driver and starts to work as an MPPT charger.
9. Observe the waveforms. Also observe that the system attempts to operate the DC power supply at the set voltage and the CC limit.
10. Increase the CC limit gradually to increase the power supplied to the battery.

6 Test Results

The following subsections describe the performance data, plots, and waveforms obtained by testing the TIDA-00476 board.

6.1 Performance Data Solar Charger

6.1.1 Efficiency at Maximum Load With Different Input Panel Voltage

Table 2. Battery Charging Performance Data—Maximum Output Power at Different Panel Voltage

V_{PANEL} (V)	I_{PANEL} (A)	V_{BAT} (V)	I_{BAT} (A)	P_{IN} (W)	P_{OUT} (W)	EFF (%)
17	4.355	14	5.03	74.04	70.42	95.1
20	3.676	14	5.01	73.52	70.14	95.4
25	2.97	14	5.06	74.49	70.84	95.1
30	2.466	14	5.1	73.98	70.14	94.8
40	1.86	14	5.03	74.43	70.42	94.6

6.1.2 Efficiency With Load Variation With Fixed Input Panel Voltage

Table 3. Battery Charging Performance Data—Different Output Power at Fixed Panel Voltage

V_{PANEL} (V)	V_{BAT} (V)	I_{BAT} (V)	P_{IN} (W)	P_{OUT} (W)	EFF (%)
17	12.7	0.104	1.43	1.33	91.8
17	12.76	0.635	8.4	8.1	96.4
17	12.8	0.957	12.25	11.41	93
17	12.9	1.79	24.26	23.17	95.3
17	12.95	3.071	41.85	39.76	95
17	13	4.009	55.09	52.17	94.6
17	13.1	5.05	69.61	65.65	94.3

6.2 Performance Data CC-CV Driver

6.2.1 Efficiency at Maximum Load Current Operating in CC Region versus Load Voltage

Table 4. CC-CV Driver Performance Data—Different Output Load Voltage at Fixed Load Current

V_{BAT} (V)	I_{BAT} (A)	V_{LOAD} (V)	I_{LOAD} (A)	P_{IN} (W)	P_{OUT} (W)	EFF (%)
12.15	1.695	27.25	0.696	20.59	18.97	92.1
12.13	1.896	30.37	0.693	23.00	21.05	91.5
12.12	2.034	32.29	0.699	22.57	24.65	91.6
12.11	2.311	36.23	0.706	25.58	27.99	91.6
12.09	2.577	40.37	0.702	28.34	31.16	90.9

6.2.2 Efficiency in CV Region for Different Load Currents

Table 5. CC-CV Driver Performance Data—Different Load Current at Fixed Load Voltage

V_{BAT} (V)	I_{BAT} (A)	V_{LOAD} (V)	I_{LOAD} (A)	P_{IN}(W)	P_{OUT} (W)	EFF (%)
32.01	0.298	12.6	0.83	9.54	10.46	91.2
32	0.41	12.58	1.13	13.12	14.22	92.3
32.05	0.5	12.68	1.37	16.03	17.37	92.3
32.03	0.65	12.56	1.81	20.82	22.73	91.6
32.1	0.689	12.56	1.93	22.12	24.24	91.3

6.3 Performance Curves Solar Charger

The following Figure 20 and Figure 21 show the efficiency of a solar charger in different panel voltage and battery current conditions.

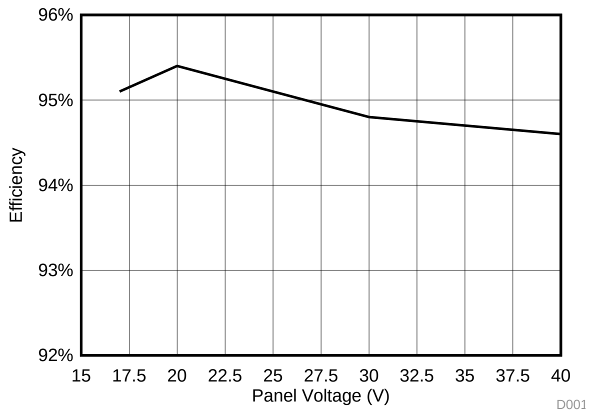

Figure 20. Variation of Solar Charger Efficiency With Panel Voltage at Maximum Battery Charging Current

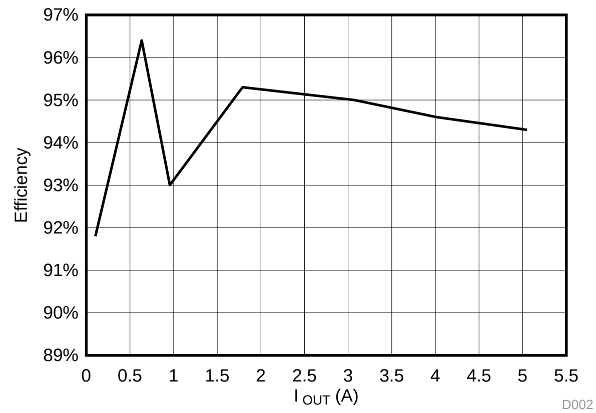

Figure 21. Efficiency Variation With Battery Charging Current

6.4 Performance Curves CC-CV Driver

Figure 22 shows the efficiency of the CC-CV driver when operating in the CV region under different load currents with a fixed load voltage of 32 V. Figure 23 shows the efficiency of the CC-CV driver when operating in the CC region under a fixed load current of 0.7 A and varying load voltage. Figure 24 shows the load current regulation when operating in the CC region under different load voltages.

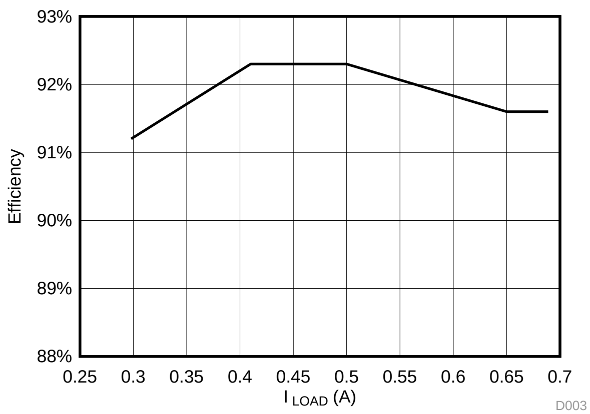

Figure 22. Efficiency Variation With DC Load Current Variation in CV Mode

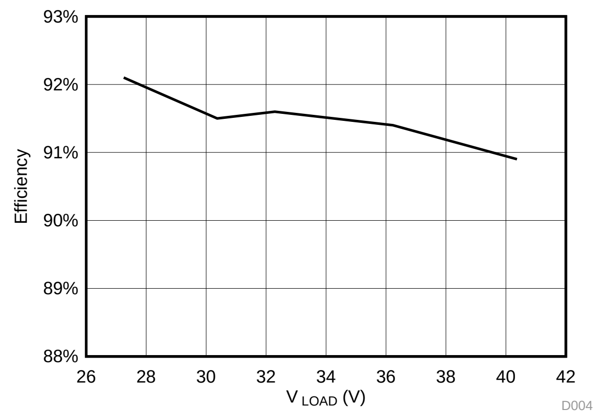

Figure 23. Efficiency Variation With DC Load Voltage Variation in CC Mode

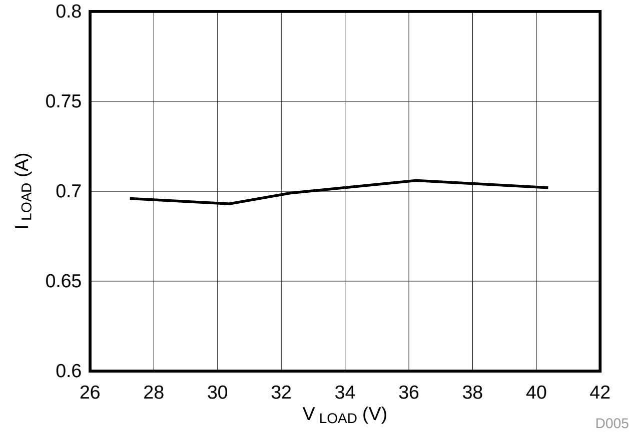

Figure 24. CC Current Regulation With Different Load Voltage

6.5 *Performance Waveform*

This subsection contains the functional waveforms that have been observed when testing the TIDA-00476 board.

One of the key waveforms in this system is the complementary PWM generated to drive the power stage. The complementary PWM is generated by the MSP430F5132 with sufficient dead time between the two signals.

The complementary PWM output is captured at the pins of the LM5109A gate driver, which the following Figure 25 shows.

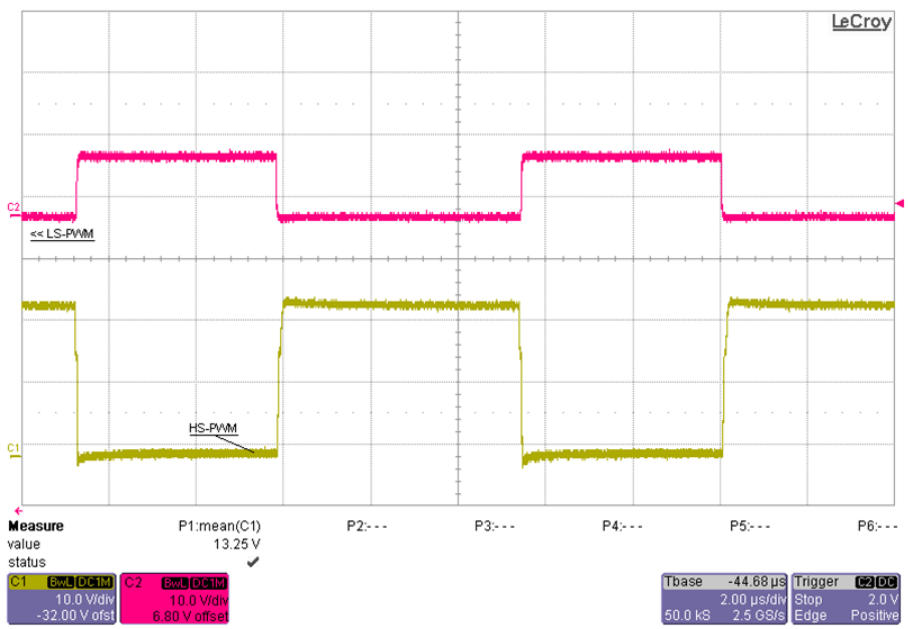

Figure 25. Complementary PWM Output from LM5109A Gate Driver

Figure 26 shows a zoomed-in image of the waveform with the complementary PWM outputs.

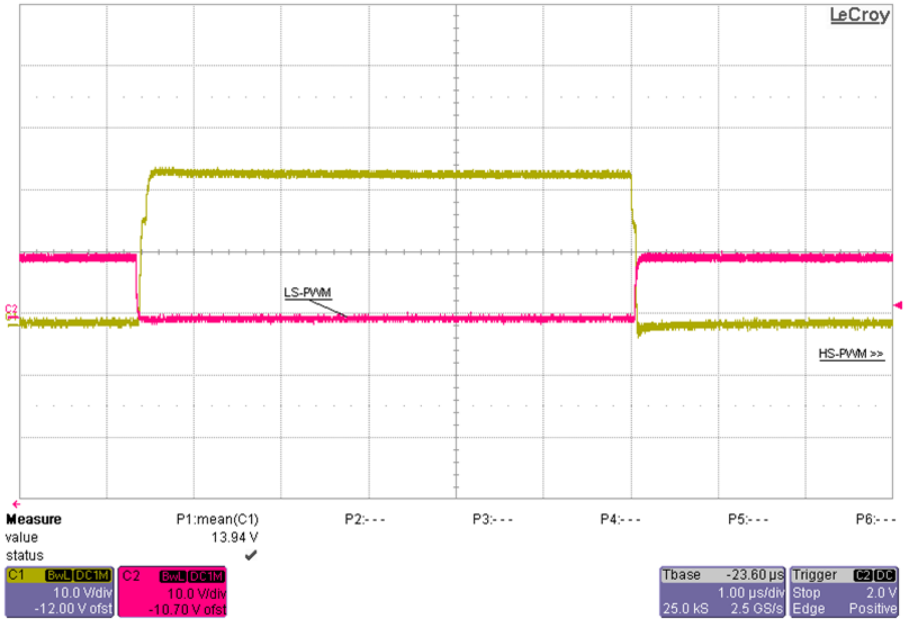

Figure 26. Complementary PWM Output From LM5109A Zoomed-In to Show Dead Time

The following Figure 27 shows the switching node waveform when the TIDA-00476 board is working as a battery charger. This waveform has been observed when the panel voltage is at 20 V and the charging current is at the maximum 5 A.

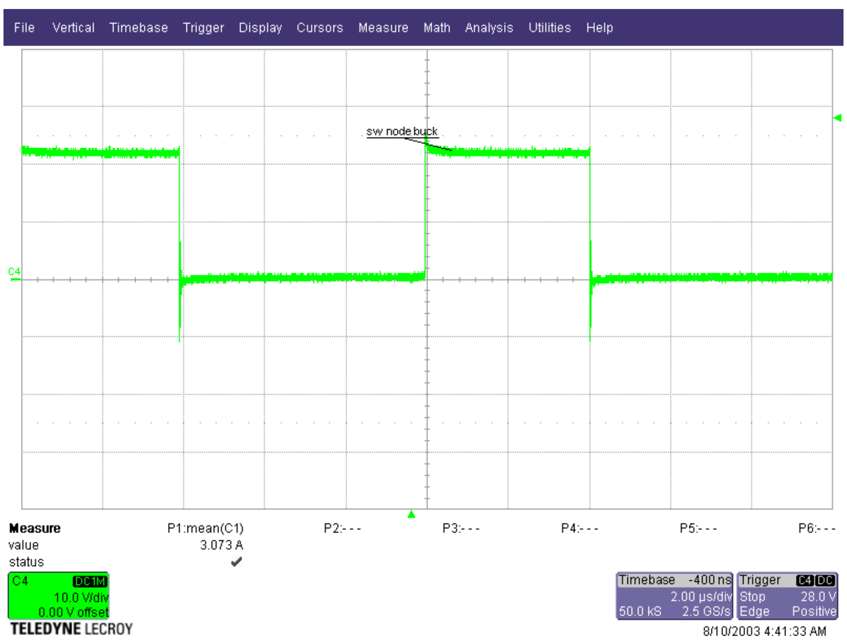

Figure 27. Switching Node Waveform When System is Working as Synchronous Buck Battery Charger

The following Figure 28 shows the battery-charging startup waveform, where the battery current ramps up from 0 A. The designer can observe that the battery current ramps up from 0 A to the current determined by the MPP of the solar panel. Because of the P&O MPPT algorithm, the operating point continues to oscillate around this MPP. From the following waveform, the designer can see that this is the oscillation in the battery charging current.

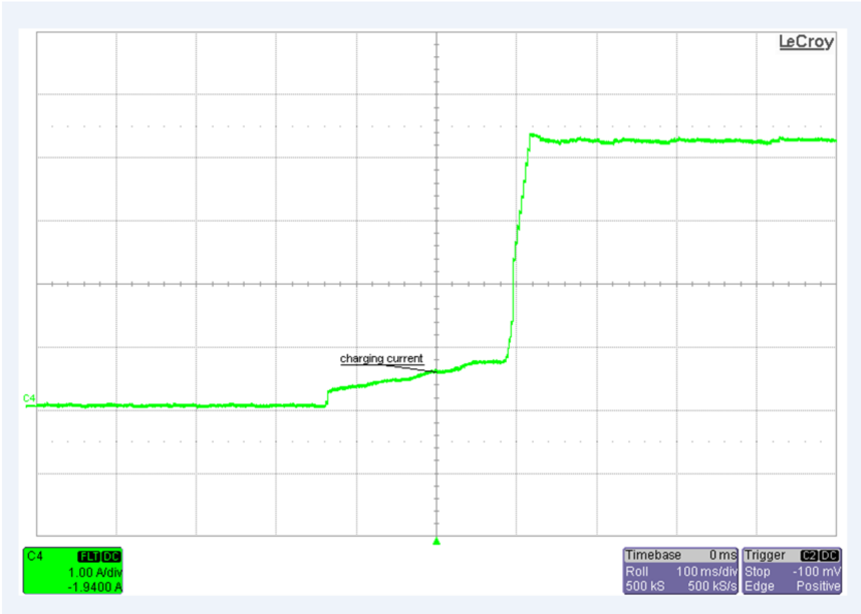

Figure 28. Ramp Up of Battery Charging Current and MPPT Action

As Section 4.1 explains, while operating as a battery charger, the power stage moves between the diode emulation and synchronous buck modes depending on the battery charging current. When the current is greater than 1 A, the power stage operates in synchronous buck mode and when the power stage is less than 1 A, the power stage operates in diode emulation mode. The following Figure 29 captures this behavior.

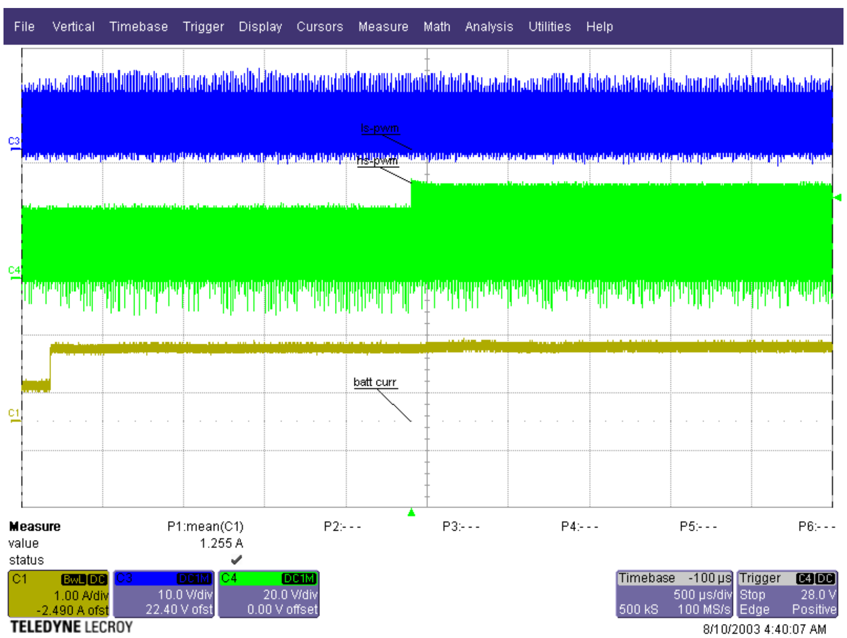

Figure 29. Change in Power Stage Operating Mode From Diode Emulation to Synchronous Buck

In the preceding Figure 29, the designer can see that after the battery current reaches close to 1 A, within a few milliseconds the power stage changes from buck mode to synchronous buck mode. In the following Figure 30 the transition point has been captured to depict the gate driver waveforms, when the transition occurs.

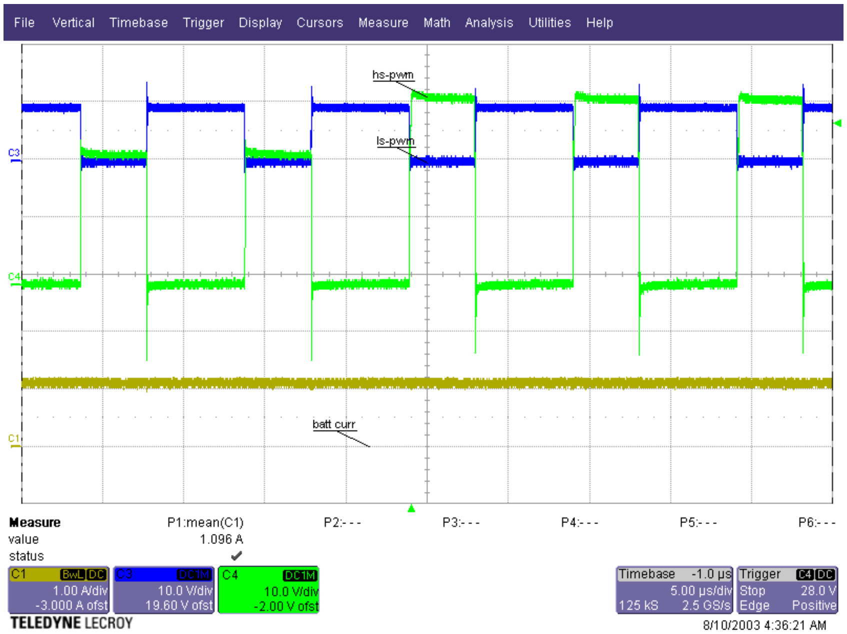

Figure 30. LM5109A PWM Output Change When Power Stage Transitions From Diode Emulation Mode to Synchronous Buck Mode

The following Figure 31 shows the switching node waveform when the TIDA-00476 board is working as a CC-CV driver. The battery voltage has been set to 12 V and the CC-CV driver output voltage 44 V. The waveform has been captured when the load current is at 0.7 A.

Figure 31. Switching Node Waveform When System is Operating as Synchronous Boost CC-CV Driver

The following Figure 32 shows the output of the CC-CV driver as the load voltage and load current ramp up is captured. This figure also shows the soft start behavior of the CC-CV driver at startup.

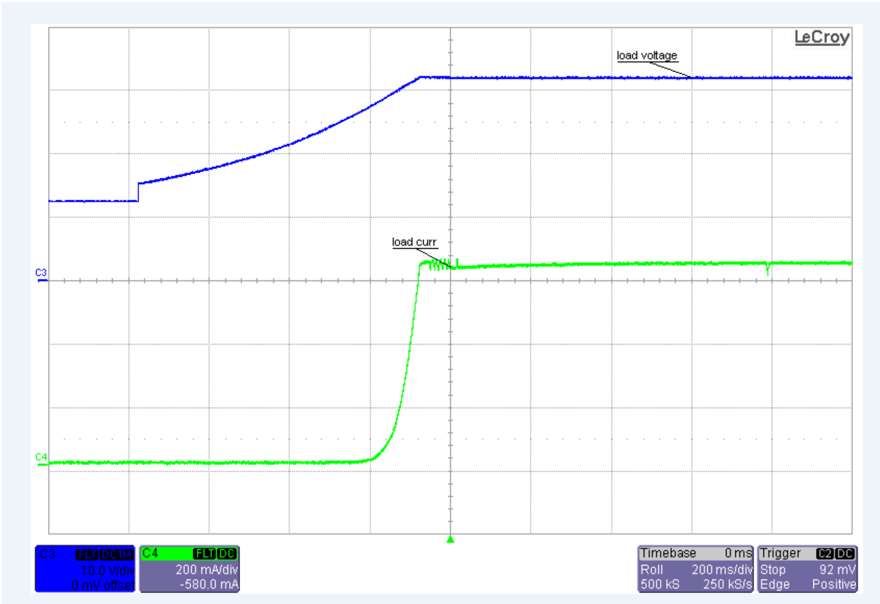

Figure 32. Ramp Up of CC-CV Driver Voltage and Current

The following Figure 33 shows the current ripple in the load current when the CC-CV driver is operating the CC region.

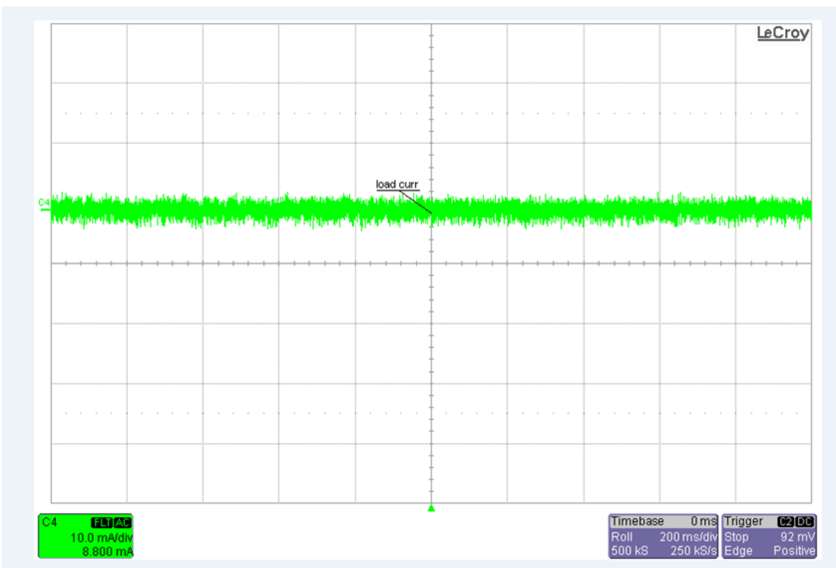

Figure 33. Current Ripple of CC-CV Driver Output Load When Operating in CC Region

6.6 Thermal Measurements

Thermal images are plotted at room temperature (25°C) within an enclosure, with no airflow, and at full load conditions. The board runs for 30 minutes before capturing the thermal image.

The images in the following Figure 34 and Figure 35 have been taken after running the board by connecting a 17-V supply at the DC input terminals and charging a 12-V battery with a 5-A current.

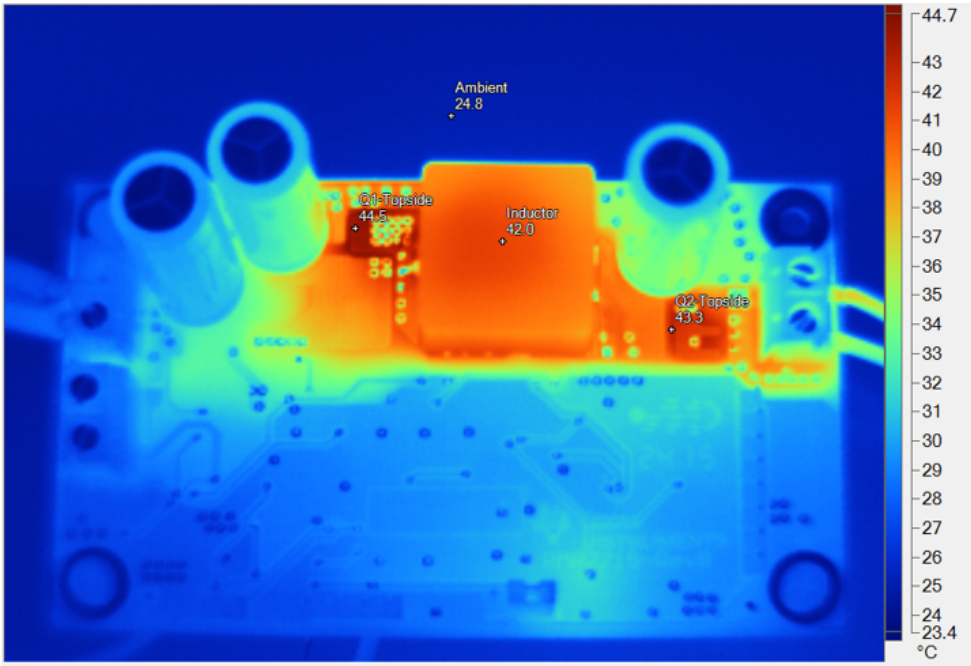

Figure 34. TIDA-00476 Thermal Image of Board—Top Side

Table 6. Highlighted Image Markers—Figure 34

NAME	TEMPERATURE
Ambient	24.8°C
Q1 top side	44.5°C
Q2 top side	43.3°C
Inductor	42.0°C

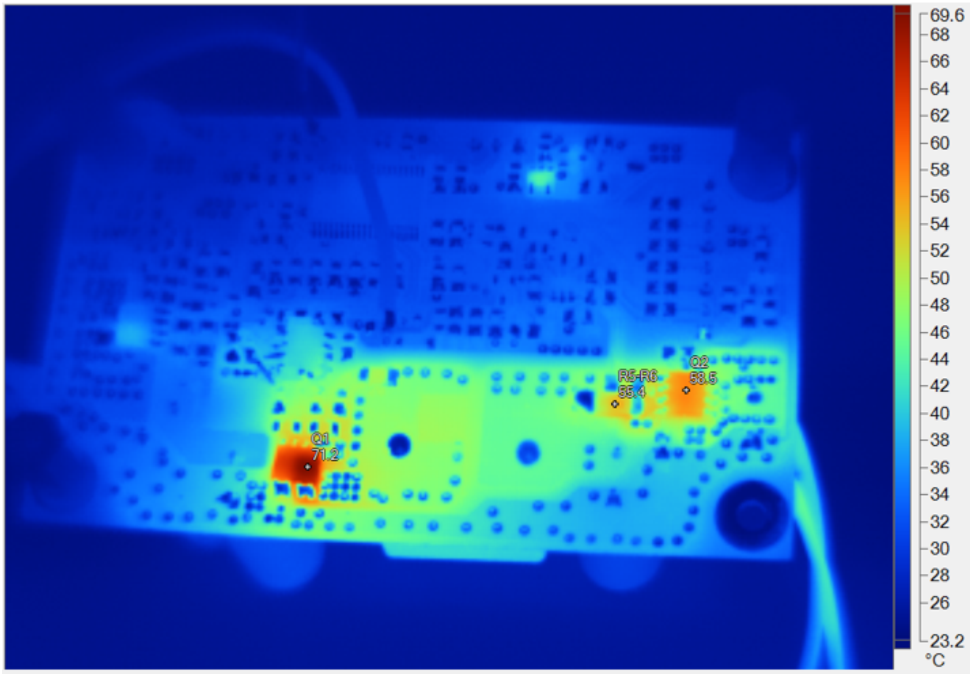

Figure 35. TIDA-00476 Thermal Image of Board—Bottom Side

Table 7. Highlighted Image Markers—Figure 35

NAME	TEMPERATURE
Q1 bottom side	71.2°C
Q2 top side	58.5°C
Sense resistor R5 and R6	55.4°C

7 Design Files

7.1 Schematics

To download the schematics for each board, see the design files at TIDA-00476.

7.2 Bill of Materials

To download the bill of materials (BOM), see the design files at TIDA-00476.

7.3 PCB Layout Recommendations

7.3.1 Power Stage Layout Guidelines

1. Keep the main switching loop comprising of capacitors C1, C2, C2, inductor L1 and MOSFET Q1 as short as possible.
2. Use a copper pour below the drains of the Q1A and Q1B MOSFETs. Also, place a sufficient number of thermal vias, which helps to dissipate heat from the dual MOSFET Q1.
3. Place the snubber component R7, R58, and C7 close to the MOSFET Q1.
4. Place the diode D7 close to the HS pin of the LM5109A.

7.3.2 Layout Prints

To download the layout prints for each board, see the design files at TIDA-00476.

7.4 Gerber Files

To download the Gerber files for each board, see the design files at TIDA-00476.

7.5 Assembly Drawings

To download the assembly drawings for each board, see the design files at TIDA-00476.

8 Software Files

To download the software files, see the design files at TIDA-00476.

9 References

1. Texas Instruments, *Test Report of MPPT Charge Controller PMP7605*, TIDA-00120 Test Results (TIDU219)
2. Tsai, C.-T.; Kuo, Y.-C.; Kuo, Y.-P.; Hsieh, C.-T. *A Reflex Charger with ZVS and Non-Dissipative Cells for Photovoltaic Energy Conversion*. Energies 2015, 8, 1373-1389.

10 About the Author

RAMKUMAR S is a Systems Engineer at Texas Instruments, where he is responsible for developing reference design solutions for the industrial segment. Ramkumar brings to this role his diverse experience in analog and digital power supplies design. Ramkumar earned his Master of Technology (M.Tech) from Indian Institute of Technology, Delhi.

IMPORTANT NOTICE FOR TI REFERENCE DESIGNS

Texas Instruments Incorporated ("TI") reference designs are solely intended to assist designers (“Buyers”) who are developing systems that incorporate TI semiconductor products (also referred to herein as “components”). Buyer understands and agrees that Buyer remains responsible for using its independent analysis, evaluation and judgment in designing Buyer’s systems and products.

TI reference designs have been created using standard laboratory conditions and engineering practices. **TI has not conducted any testing other than that specifically described in the published documentation for a particular reference design.** TI may make corrections, enhancements, improvements and other changes to its reference designs.

Buyers are authorized to use TI reference designs with the TI component(s) identified in each particular reference design and to modify the reference design in the development of their end products. HOWEVER, NO OTHER LICENSE, EXPRESS OR IMPLIED, BY ESTOPPEL OR OTHERWISE TO ANY OTHER TI INTELLECTUAL PROPERTY RIGHT, AND NO LICENSE TO ANY THIRD PARTY TECHNOLOGY OR INTELLECTUAL PROPERTY RIGHT, IS GRANTED HEREIN, including but not limited to any patent right, copyright, mask work right, or other intellectual property right relating to any combination, machine, or process in which TI components or services are used. Information published by TI regarding third-party products or services does not constitute a license to use such products or services, or a warranty or endorsement thereof. Use of such information may require a license from a third party under the patents or other intellectual property of the third party, or a license from TI under the patents or other intellectual property of TI.

TI REFERENCE DESIGNS ARE PROVIDED "AS IS". TI MAKES NO WARRANTIES OR REPRESENTATIONS WITH REGARD TO THE REFERENCE DESIGNS OR USE OF THE REFERENCE DESIGNS, EXPRESS, IMPLIED OR STATUTORY, INCLUDING ACCURACY OR COMPLETENESS. TI DISCLAIMS ANY WARRANTY OF TITLE AND ANY IMPLIED WARRANTIES OF MERCHANTABILITY, FITNESS FOR A PARTICULAR PURPOSE, QUIET ENJOYMENT, QUIET POSSESSION, AND NON-INFRINGEMENT OF ANY THIRD PARTY INTELLECTUAL PROPERTY RIGHTS WITH REGARD TO TI REFERENCE DESIGNS OR USE THEREOF. TI SHALL NOT BE LIABLE FOR AND SHALL NOT DEFEND OR INDEMNIFY BUYERS AGAINST ANY THIRD PARTY INFRINGEMENT CLAIM THAT RELATES TO OR IS BASED ON A COMBINATION OF COMPONENTS PROVIDED IN A TI REFERENCE DESIGN. IN NO EVENT SHALL TI BE LIABLE FOR ANY ACTUAL, SPECIAL, INCIDENTAL, CONSEQUENTIAL OR INDIRECT DAMAGES, HOWEVER CAUSED, ON ANY THEORY OF LIABILITY AND WHETHER OR NOT TI HAS BEEN ADVISED OF THE POSSIBILITY OF SUCH DAMAGES, ARISING IN ANY WAY OUT OF TI REFERENCE DESIGNS OR BUYER’S USE OF TI REFERENCE DESIGNS.

TI reserves the right to make corrections, enhancements, improvements and other changes to its semiconductor products and services per JESD46, latest issue, and to discontinue any product or service per JESD48, latest issue. Buyers should obtain the latest relevant information before placing orders and should verify that such information is current and complete. All semiconductor products are sold subject to TI’s terms and conditions of sale supplied at the time of order acknowledgment.

TI warrants performance of its components to the specifications applicable at the time of sale, in accordance with the warranty in TI’s terms and conditions of sale of semiconductor products. Testing and other quality control techniques for TI components are used to the extent TI deems necessary to support this warranty. Except where mandated by applicable law, testing of all parameters of each component is not necessarily performed.

TI assumes no liability for applications assistance or the design of Buyers’ products. Buyers are responsible for their products and applications using TI components. To minimize the risks associated with Buyers’ products and applications, Buyers should provide adequate design and operating safeguards.

Reproduction of significant portions of TI information in TI data books, data sheets or reference designs is permissible only if reproduction is without alteration and is accompanied by all associated warranties, conditions, limitations, and notices. TI is not responsible or liable for such altered documentation. Information of third parties may be subject to additional restrictions.

Buyer acknowledges and agrees that it is solely responsible for compliance with all legal, regulatory and safety-related requirements concerning its products, and any use of TI components in its applications, notwithstanding any applications-related information or support that may be provided by TI. Buyer represents and agrees that it has all the necessary expertise to create and implement safeguards that anticipate dangerous failures, monitor failures and their consequences, lessen the likelihood of dangerous failures and take appropriate remedial actions. Buyer will fully indemnify TI and its representatives against any damages arising out of the use of any TI components in Buyer’s safety-critical applications.

In some cases, TI components may be promoted specifically to facilitate safety-related applications. With such components, TI’s goal is to help enable customers to design and create their own end-product solutions that meet applicable functional safety standards and requirements. Nonetheless, such components are subject to these terms.

No TI components are authorized for use in FDA Class III (or similar life-critical medical equipment) unless authorized officers of the parties have executed an agreement specifically governing such use.

Only those TI components that TI has specifically designated as military grade or “enhanced plastic” are designed and intended for use in military/aerospace applications or environments. Buyer acknowledges and agrees that any military or aerospace use of TI components that have ***not*** been so designated is solely at Buyer's risk, and Buyer is solely responsible for compliance with all legal and regulatory requirements in connection with such use.

TI has specifically designated certain components as meeting ISO/TS16949 requirements, mainly for automotive use. In any case of use of non-designated products, TI will not be responsible for any failure to meet ISO/TS16949.

Mailing Address: Texas Instruments, Post Office Box 655303, Dallas, Texas 75265